

PSFC/JA-01-8

**Beam Confinement in Periodic
Permanent Magnet Focusing Klystrons**

M. Hess and C. Chen

April 2001

Plasma Science and Fusion Center
Massachusetts Institute of Technology
Cambridge, MA 02139, USA

This work was supported by the Department of Energy, Office of High Energy and Nuclear Physics, Grant No. DE-FG02-95ER-40919, and by the Air Force Office of Scientific Research, Grant No. F49620-00-1-0007. Reproduction, translation, publication, use and disposal, in whole or part, by or for the United States government is permitted.

Submitted for publication in *Physical Review Letters*.

BEAM CONFINEMENT IN PERIODIC PERMANENT MAGNET FOCUSING KLYSTRONS

Mark Hess and Chiping Chen
Plasma Science and Fusion Center
Massachusetts Institute of Technology
Cambridge, Massachusetts 02139

ABSTRACT

The confinement of a tightly bunched electron beam is studied in a periodic permanent magnet (PPM) focusing klystron. By analyzing the Hamiltonian dynamics of a train of collinear periodic point charges interacting with a conducting drift tube, an rf field, and an applied PPM focusing field, a space-charge limit is derived for the radial confinement of lightly bunched electron beams, and is shown to be significantly below the well-known Brillouin density limit for an unbunched beam. Several state-of-the-art PPM klystrons developed at SLAC are found to operate close to this limit, shedding some light on the origin of observed beam losses.

PACS: 29.27, 41.85

The confinement of intense charged-particle beams is an important subject in beam physics [1] and plasma physics [2]. It is critical to the research and development of high-intensity rf and induction linacs and high-intensity storage rings for high-energy and nuclear physics research, spallation neutron sources, and heavy ion fusion [3]. The confinement of intense electron beams is also important to the development of high-power microwave (HPM) sources [4], such as klystrons, traveling wave tubes and backward wave oscillators. One of the main challenges for successful operation of these devices at high-intensities, which is related to beam confinement, is the prevention of beam halo formation [5,6] and beam loss. Recently, beam losses have been measured in a number of high-intensity accelerator and high-power microwave experiments. For example, beam power losses have been observed in several periodic permanent magnet (PPM) focusing klystrons [7] at the Stanford Linear Accelerator Center and in other HPM sources elsewhere [8]. Beam loss has also been attributed to be a limiting factor in the proton storage ring (PSR) [9] at Los Alamos and in the relativistic heavy ion collider (RHIC) [10] at Brookhaven. While the physics of confining continuous charged beams has been studied extensively in plasma physics [2] and vacuum electronics [4], the confinement properties of bunched beams, like those used in the SLAC PPM klystrons and other high-intensity rf accelerators, have only had modest investigation [11-13].

In this Letter, we show the existence of a theoretical space-charge limit for confining bunched electron beams in high-power PPM focusing klystrons. High-power klystron amplifiers are ideal devices for studying the three-dimensional effects of beam-wall interactions on the confinement of bunched beams, since high-intensity beam bunches must travel a relatively long distance through a conducting drift tube whose radius must be small enough to prevent second harmonic propagation. The present self-field parameter limit is an extension of, but is well below, the well-known Brillouin density limit [2,14], $2\mathbf{w}_p^2/\mathbf{w}_c^2 = 1$, which is applicable to continuous beams in a uniform-focusing magnetic field of $B\hat{\mathbf{e}}_z$ in the rest frame of the beam. Here, $\mathbf{w}_p = (4\pi n_e e^2/m_e)^{1/2}$ and $\mathbf{w}_c = eB/m_e c$ are the plasma and cyclotron frequencies, respectively, in cgs units. As an important application, we will apply the present beam confinement criterion to two state-of-the-art X-band PPM focusing klystrons [7,15] developed at SLAC for the Next Linear

Collider (NLC) and the W-band Klystrino [16], another PPM device at SLAC. We will show that the self-field parameters for these devices are close to the limit, which sheds some light on the origin of beam losses observed in these devices.

The present model begins with a relativistic Hamiltonian description of a collinear periodic distribution of electron bunches moving in a perfectly conducting cylindrical pipe of radius a . The electrons are focused transversely by an applied PPM focusing field. Assuming that the beam is strongly bunched longitudinally by an rf field, and has a negligibly small transverse size, we approximate the beam bunches by periodic point charges with a periodic spacing of L . In terms of klystron parameters, L corresponds to v_b/f , where $v_b = \mathbf{b}_b c$ is the average velocity of the bunches moving parallel to the pipe axis, and f is the operating frequency of the klystron. Figure 1 shows a diagram of the system.

Since the electron bunches are collinear and periodic, we only need to specify the coordinates of the center of mass of one electron bunch in the Hamiltonian. In the externally applied magnetic field $\mathbf{B}^{ext} = \nabla \times \mathbf{A}^{ext}$ with $\mathbf{A}^{ext} = (rB_0/2)\cos(k_0z)\hat{\mathbf{e}}_q$ and the approximated rf field $E\cos(kz - \mathbf{w}t)\hat{\mathbf{e}}_z$ with $k = 2\mathbf{p}/L$ and $\mathbf{w} = 2\mathbf{p}f$ being the wave number and angular frequency, the Hamiltonian for this system is given in the laboratory frame by

$$H = \left[M^2 c^4 + c^2 P_r^2 + (cP_z - QA_z^{self})^2 + \left(\frac{cP_q}{r} - QA_q^{ext} \right)^2 \right]^{1/2} + Q\mathbf{f}^{self} - \frac{QE}{k} \sin(kz - \mathbf{w}t), \quad (1)$$

where $Q = -Ne$ is the total charge of an electron bunch, $M = Nm_e$ is the total mass of the electron bunch, N is the number of electrons per bunch, $-e$ and m_e are the electron charge and rest mass, respectively, \mathbf{P} is the canonical momentum of the electron bunch, \mathbf{f}^{self} and \mathbf{A}^{self} are the scalar and vector potentials associated with the charge and current on the conductor wall induced by the beam itself, respectively, and c is the speed of light in vacuum. In expressing Eq. (1), we have implicitly assumed that $v_b \gg |v_q|$ and $v_b \gg |v_r|$, which is consistent with the fact that the axial motion remains relativistic, and the usual assumption that the effective Budker parameter is small, or more specifically,

$Ne^2/m_e c^2 L \ll a/L$. Consequently, $\mathbf{A}^{self} \equiv A_z^{self} \hat{\mathbf{e}}_z$. Consistent with the assumptions $v_b \gg |v_\theta|$ and $v_b \gg |v_r|$, it will be shown shortly that $A_z^{self} \equiv \mathbf{b}_b \mathbf{f}^{self}$.

In order to find the self-field potentials, A_z^{self} and \mathbf{f}^{self} , it is useful to momentarily transform to the rest frame of the beam, using the property that the scalar and vector potentials form 4-vectors, $(\mathbf{f}_{rest}^{self}, \mathbf{A}_{rest}^{self})$ and $(\mathbf{f}^{self}, \mathbf{A}^{self})$, in the rest and laboratory frames, respectively. Since there is no longitudinally induced current on the conductor surface in the rest frame, $\mathbf{A}_{rest}^{self} = 0$. The beam-wall interaction becomes purely electrostatic in the rest frame, and \mathbf{f}_{rest}^{self} may be calculated by solving Poisson's equation. In a previous paper [13], the authors utilized a Green's function approach to compute the electrostatic potential \mathbf{f}_{rest}^{self} . The Green's function was constructed from an eigenmode expansion over the three-dimensional solutions that solve Poisson's equation for the cylindrical conductor geometry. By using the Green's function, the induced surface charge density was computed, and the electrostatic potential \mathbf{f}_{rest}^{self} due to the induced charge was obtained. The result is given by [13]

$$\mathbf{f}_{rest}^{self}(r) = \frac{Q}{L_{rest}} \left[\ln(\mathbf{a}^2 - \hat{r}^2) - 2 \sum_{n=1}^{\infty} K_0(n\mathbf{a}) I_0^2(n\hat{r}) / I_0(n\mathbf{a}) - 4 \sum_{n=1}^{\infty} \sum_{l=1}^{\infty} K_l(n\mathbf{a}) I_l^2(n\hat{r}) / I_l(n\mathbf{a}) \right]. \quad (2)$$

Here, $L_{rest} = \mathbf{g}_b L$ is the rest-frame bunch spacing, $\mathbf{g}_b = (1 - \mathbf{b}_b^2)^{-1/2}$, $\hat{r} = 2\mathbf{p}r/L_{rest}$, $\mathbf{a} = 2\mathbf{p}a/L_{rest}$, and $I_l(x)$ and $K_l(x)$ are the l th-order modified Bessel functions of the first and second kind, respectively. Using the Lorentz transformation, we find that $\mathbf{f}^{self} = \mathbf{g}_b \mathbf{f}_{rest}^{self}$ and $\mathbf{A}^{self} = \mathbf{g}_b \mathbf{b}_b \mathbf{f}_{rest}^{self} \hat{\mathbf{e}}_z = \mathbf{b}_b \mathbf{f}^{self} \hat{\mathbf{e}}_z$.

In the analysis of the radial confinement of the orbit of an electron bunch, we perform the canonical transformation $z' = z - v_{ph}t = \partial F_2 / \partial P_{z'}$, $P_{z'} = P_z = \partial F_2 / \partial z$, and $H' = H + \partial F_2 / \partial t$ with the generating function $F_2(z; P_{z'}, t) = (z - v_{ph}t)P_{z'}$, where $v_{ph} = \mathbf{w}/k$ is the phase velocity of the rf field. Expanding the new Hamiltonian H' with small transverse energy, we separate the nonrelativistic transverse motion from the relativistic longitudinal motion, i.e.,

$$H' = H'_{\parallel} + H'_{\perp}, \quad (3)$$

$$H'_{\parallel}(z', P_{z'}) = \mathbf{g}(P_{z'})Mc^2 - v_{ph}P_{z'} - \frac{QE}{k} \sin(kz'), \quad (4)$$

$$H'_{\perp} = \frac{1}{2\mathbf{g}(P_{z'})M} \left[P_r^2 + \left(\frac{P_q}{r} - \frac{Q}{c} A_q^{ext} \right)^2 \right] + \frac{Q}{\mathbf{g}^2(P_{z'})} \mathbf{f}^{self}, \quad (5)$$

where $\mathbf{g}(P_{z'}) = (1 + P_{z'}^2 / M^2 c^2)^{1/2}$, $A_q^{ext} = (rB_0/2) \cos[k_0(z' + v_{ph}t)]$, and use has been made of $A_z^{self} = (P_{z'} / \mathbf{g}Mc) \mathbf{f}^{self}$ for an electron bunch deeply trapped in the rf wave field.

The longitudinal dynamics described by H'_{\parallel} in Eq. (4) is readily determined. In particular, the bounce frequency is $\omega_B = (EkQ / \mathbf{g}_b^3 M)^{1/2}$ for an electron bunch deeply trapped in the rf wave field at $kz' = (4n+1)\mathbf{p} / 2$ with $v_z = v_b = v_{ph}$, where n is an integer. Typically, the bounce frequency is comparable to the operating rf frequency.

For the deeply trapped electron bunch, the transverse motion occurs on a time scale that is long compared with the beam transit time through one period of the PPM focusing field. The Hamiltonian H'_{\perp} for the transverse motion can be further simplified by averaging over one period of the PPM focusing field. This gives

$$\langle H'_{\perp} \rangle(r, P_r, P_q) = \frac{1}{2\mathbf{g}_b M} \left(P_r^2 + \frac{P_q^2}{r^2} + \frac{Q^2 B_{rms}^2}{4c^2} r^2 \right) + \frac{Q}{\mathbf{g}_b^2} \mathbf{f}^{self}, \quad (6)$$

where $\langle H'_{\perp} \rangle = (2\mathbf{p})^{-1} \int_0^{2\mathbf{p}/k_0} k_0 dz H'_{\perp}$, $B_{rms} = B_0 / \sqrt{2}$ is the rms value of the PPM focusing field, and use has been made of $P_{z'} = \mathbf{g}_b \mathbf{b}_b Mc$. It follows from Eq. (6) that the radial equations of motion for the deeply trapped electron bunch averaged over one period of the PPM focusing field are

$$\frac{dr}{dt} = \frac{P_r}{\mathbf{g}_b M}, \quad (7)$$

$$\frac{dP_r}{dt} = \frac{1}{\mathbf{g}_b} \left[\frac{P_q^2}{Mr^3} - \frac{Q^2 B_{rms}^2 r}{4Mc^2} - \frac{Q}{\mathbf{g}_b} \frac{\partial \mathbf{f}^{self}}{\partial r} \right]. \quad (8)$$

Because $\langle H'_{\perp} \rangle = const.$, we have $P_r^2 = P_{r0}^2 + F(r_0) - F(r)$, where the subscript zero denotes the initial conditions, and $F(r) = P_q^2 / Mr^2 + Q^2 B_{rms}^2 r^2 / 4Mc^2 + 2MQ \mathbf{f}_{rest}^{self}$ is an effective radial potential. To determine the condition for radial confinement, we are only

interested in orbits near the center of the conductor, i.e. where the beam-wall interaction is weakest. Therefore, by taking the limit of the effective radial potential $F(r)$ as $r \rightarrow 0$ ($P_q = 0$) and finding the criterion that $F(r)$ is increasing, we obtain the space charge limit for radially confined orbits,

$$\frac{8c^2 I_b}{\mathbf{w}_{c,rms}^2 a^2 I_A} \leq \left[1 + \sum_{n=1}^{\infty} \frac{n\mathbf{a}}{I_0(n\mathbf{a})I_1(n\mathbf{a})} \right]^{-1}, \quad (9)$$

where $I_b = Nef$ is the average current in the klystron (in amperes), $I_A = \mathbf{g}_b \mathbf{b}_b m_e c^3 / e \cong \mathbf{g}_b \mathbf{b}_b \times 17 \text{ kA}$ is the electron Alfvén current, $\mathbf{w}_{c,rms} = eB_{rms} / m_e c$, and $\mathbf{a} = 2pa_f / \mathbf{g}_b \mathbf{b}_b c$. We note that the left-hand side of Eq. (9) is equal to the self-field parameter $2\mathbf{w}_p^2 / \mathbf{w}_{c,rms}^2$ in the rest frame, where $\mathbf{w}_p^2 = (4pe^2 / m_e)(N / pa^2 L_{rest})$ is the effective plasma frequency squared. This self-field parameter limit is similar to a limit that the authors computed for a uniform-focusing magnetic field, $\mathbf{B}^{ext} = B\hat{\mathbf{e}}_z$ [13]. The only difference is that the rms magnetic field on the left-hand side of Eq. (9) should be replaced by B . Figure 2 shows a plot of the right-hand side of Eq. (9) versus the parameter \mathbf{a} .

In the limit where the bunch spacing is small compared to the pipe radius, i.e. $\mathbf{a} \gg 1$, the system resembles a continuous beam. Equation (9) becomes $2\mathbf{w}_p^2 / \mathbf{w}_{c,rms}^2 \leq 1 - 8\mathbf{p}^3 a^2 \mathbf{g}_b^{-2} L^{-2} e^{-4pa/\mathbf{g}_b L}$, and recovers the Brillouin density limit for PPM focusing. However, the more relevant limit for high-power klystrons is when the bunch spacing is much larger than the pipe radius, i.e., $\mathbf{a} \ll 1$. Numerical analysis shows that equation (6) becomes $2\mathbf{w}_p^2 / \mathbf{w}_{c,rms}^2 \leq 2a / \mathbf{g}_b L$, which is much less than the Brillouin density limit.

We now apply the beam confinement condition in Eq. (9) to three recent PPM focusing klystron experiments at SLAC, namely, the X-band 50 MW XL-PPM and 75 MW XP klystrons [7,15] and the W-band Klystrino [16]. The parameters for all three klystrons are listed in Table 1, and their operating points are marked with letter a, b and c in Fig. 2, respectively. The X-band klystrons were designed and tested for the NLC, whereas the W-band klystrino was designed for sub-millimeter radar applications. As shown in Fig. 2 and Table 1, all three klystrons operate in the regime of $\mathbf{a} \ll 1$ and near

the self-field parameter limit. Because the 50 MW klystron operates slightly below the confinement limit, a mild beam loss still occurs in this device [7] through beam halo formation as reported previously [6,17]. The 75-MW XP is operating outside of the confinement limit. This suggests that the 75 MW klystron has greater beam loss than its 50 MW counterpart, which is consistent with more pronounced X-ray emissions measured at the output section of the device [15]. The Klystrino design parameters fall just inside of the theoretical limit, suggesting a marginally stable beam-wall interaction.

To summarize, we presented a center-of-mass model for a tightly bunched electron beam in a periodic permanent magnet (PPM) focusing klystron. By analyzing the Hamiltonian dynamics of a train of collinear periodic point charges interacting with a conducting drift tube, an rf field, and an applied PPM focusing field, we derived a space-charge limit for the radial confinement of lightly bunched electron beams, which is significantly below the well-known Brillouin density limit for a continuous beam. We found that several state-of-the-art PPM klystrons developed at SLAC operate close to this limit, thereby shedding some light on the origin of observed beam losses. A further study of PPM confinement, which includes multi-particle simulations in each bunch, is needed to make a more accurate estimate on the amount of beam loss in klystrons.

Acknowledgement

This work was supported by the Department of Energy, Office of High Energy and Nuclear Physics, Grant No. DE-FG02-95ER-40919, and by the Air Force Office of Scientific Research, Grant No. F49620-00-1-0007. The authors wish to thank D. Sprehn and G. Scheitrum for helpful discussions.

References

1. M. Reiser, *Theory and Design of Charged-Particle Beams* (Wiley & Sons, New York, 1994).
2. R. C. Davidson, *Physics of Nonneutral Plasmas* (Addison-Wesley, Reading, MA, 1990).
3. Luccio and W. Mackay, eds., *Proceedings of the 1999 Particle Accelerator Conference* (IEEE, Piscataway, NJ, 1999), and references therein.
4. J. Benford and J. Swegle, *High Power Microwaves* (Artech, Boston, 1992).
5. R. L. Gluckstern, *Phys. Rev. Lett.* **73**, 1247 (1994).
6. C. Chen and R. Pakter, *Phys. Plasmas* **7**, 2203 (2000), and references therein.
7. D. Sprehn, G. Caryotakis, E. Jongewaard, R. M. Phillips, in *Proceedings of 19th International Linac Conference* (Argonne National Laboratory Report ANL-98/28), p. 689.
8. F. Hegeler, C. Grabowski, and E. Schamiloglu, *IEEE Trans. Plasma Sci.* **PS-26**, 275 (1998).
9. D. H. Fitzgerald, *et al.*, in Ref. 3, p. 518.
10. M. Harrison, in Ref. 3, p. 6.
11. J. J. Barnard, and S. M. Lund, in *Proceedings of the 1997 Particle Accelerator Conference* (IEEE, Piscataway, NJ, 1997), p. 1929.
12. Gluckstern, R.L., A.V., Fedotov, S. Kurennoy, and R. Ryne, *Phys. Rev.* **E58**, 4977 (1998).
13. M.Hess and C. Chen, *Phys. Plasmas* **7**, 5206 (2000).
14. L. Brillouin, *Phys. Rev.* **67**, 260 (1945).
15. D. Sprehn, G. Caryotakis, E. N. Jongewaard, R. M. Phillips, and A. Vlieks, in *Intense Microwave Pulses VII*, edited by H. E. Brandt, *SPIE Proc.* **4301**, 132 (2000).
16. G. Scheitrum, private communication (2000).
17. R. Pakter and C. Chen, *IEEE Trans. Plasma Sci.* **28**, 502 (2000).

Figure Captions

Fig. 1 Diagram of a periodic array of charges propagating in a perfectly conducting cylinder with longitudinal velocity $v_b \hat{\mathbf{e}}_z$.

Fig. 2 Plot of the maximum value of the self-field parameter (solid curve),

$8c^2 I_b / \mathbf{w}_{c,rms}^2 a^2 I_A$, for bunched beam confinement as a function of the parameter

$\mathbf{a} = 2\mathbf{p}af / \mathbf{g}_b \mathbf{b}_b c$. Shown in letters are the operating points for three PPM

focusing klystrons: a) 50 MW XL-PPM, b) 75 MW XP, and c) Klystrino. The

dashed line denotes the Brillouin density limit for an unbunched beam.

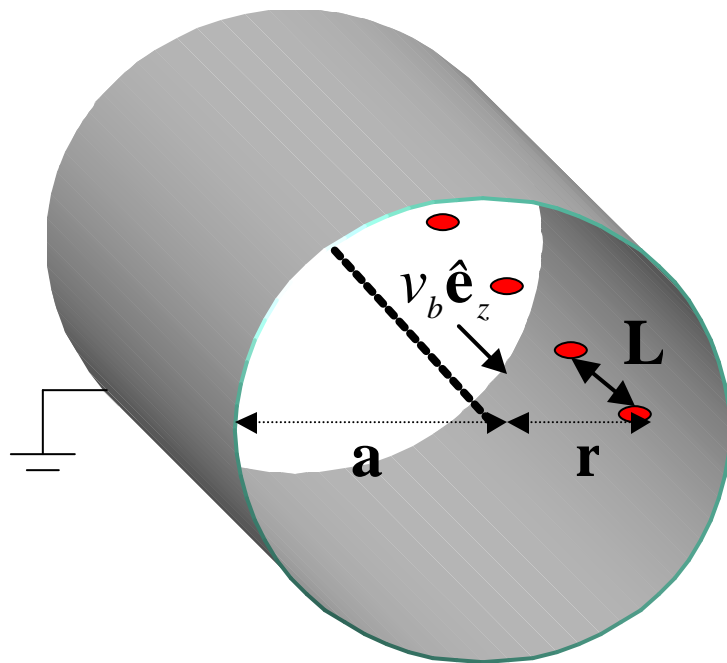


Figure 1

Hess and Chen, PRL

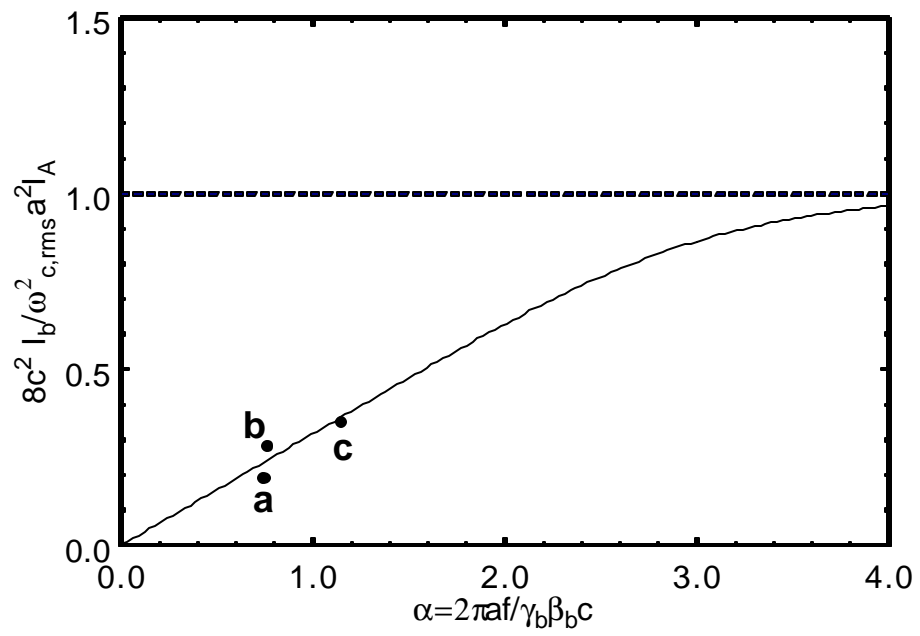


Figure 2

Hess and Chen, PRL

Table 1. Parameters for SLAC PPM Focusing Klystrons

PARAMETER	50 MW XL-PPM	75 MW XP	KLYSTRINO
f (GHz)	11.4	11.4	95
I_b (A)	190	257	2.4
g_b	1.83	1.96	1.22
B_{rms} (T)	0.20	0.16	0.29
a (cm)	0.48	0.54	0.04
\mathbf{a}	0.75	0.77	1.15
$\frac{8c^2 I_b}{w_{c,rms}^2 a^2 I_A} \Big _{exp}$	0.19	0.28	0.35
$\frac{8c^2 I_b}{w_{c,rms}^2 a^2 I_A} \Big _{cr}$	0.238	0.244	0.366